

Mechanism of the Exchanges Catalysed by the Oxoglutarate Translocator of Rat-Heart Mitochondria Kinetics of the External-Product Inhibition

Francis E. SLUSE, Georges GOFFART, and Claude LIÉBECQ

Laboratoire de Biochimie et de Physiologie Générale, Institut Supérieur d'Éducation Physique, Université de Liège

(Received July 29/September 28, 1972)

The kinetics of the exchange reactions between internal L-malate and external 2-oxoglutarate or malonate have been measured at 4 °C in the presence of external L-malate (external-product inhibitor), using preparations of rat-heart mitochondria under conditions where the oxoglutarate translocator is operating exclusively. Measurements of initial rates were made at three concentrations of the internal substrate (L-malate), three concentrations of the external substrate (2-oxoglutarate or malonate) and three concentrations of the external reaction product (L-malate).

The Michaelis constant for the internal malate is unaffected by the presence of the external product whereas the apparent-maximum rate for each concentration of external substrate decreases when the concentration of external product increases. On the other hand the Michaelis constant for the external substrate, oxoglutarate or malonate, increases when the concentration of external malate increases.

The external product inhibits the exchange in a competitive way when external substrate is varied and in a non-competitive way when internal substrate is varied.

The inhibition constant determined for the external malate is equal to the previously determined dissociation constant of the corresponding external-malate · translocator complex.

These results are in perfect agreement with the previously proposed mechanism (rapid-equilibrium random bi-bi) and a mixed dead-end and product inhibition.

The mitochondrial inner membrane contains several anion translocators catalysing exchange-diffusion reactions between intra- and extramitochondrial anions. The translocations follow a one-to-one stoichiometry [1] and the translocators show a selectivity for the anions exchanged and a specific sensitivity to inhibitors (for a review, see [2]).

Kinetic studies of such exchange reactions are available [3-8] but, except for the case of the oxoglutarate translocator of heart-muscle mitochondria [8], are of limited value and do not permit the proposal of possible mechanisms for the exchange reactions.

In most cases, the penetration of labelled substrates has been measured [3,4,7] under conditions where the nature (except [7]) and concentration of the intramitochondrial counter-ions were not known. Where the efflux of labelled anions has been measured in exchange for known external counter-ions [5,6],

it had been assumed that internal endogenous anions do not influence the efflux of the tracer anion; this is not necessarily the case.

Furthermore, except in the case of tricarboxylate translocation [7], more than one translocator participates in the exchange reaction under investigation. The parameters obtained under such conditions may not characterise a single translocator.

On the other hand, the conditions used in the kinetic study of the oxoglutarate translocator [8] lead to results which can be described in terms of dissociation constants and from which a possible exchange-reaction mechanism can be deduced [8]. The activity of a single translocator had been isolated, and a set of internal-anion concentrations had been realized.

Substrate inhibitions for dicarboxylate and tricarboxylate translocations are reported in the literature [4,7]. Kinetically speaking they are also of limited value but may be used for qualitative considerations [4].

This paper reports the results of product inhibition of the reactions catalysed by the oxoglutarate

Abbreviations. S.D., standard deviation.

Enzyme. Malate dehydrogenase, or L-malate: NAD oxidoreductase (EC 1.1.1.37).

translocator. Two of the possible exchange reactions have been measured in the presence of an external product of known concentration: (a) internal malate/external oxoglutarate in the presence of external malate, (b) internal malate/external malonate in the presence of external malate. The concentrations of internal and external substrates are known in these experiments.

The kinetic parameters have been calculated assuming an exchange reaction analogous to a two-substrate two-product enzyme-catalysed reaction.

EXPERIMENTAL PROCEDURE

Materials

Special reagents were obtained from the following sources: [2-¹⁴C]malonic acid, 2-oxo[5-¹⁴C]glutarate, [U-¹⁴C]sucrose and tritiated water (The Radiochemical Center, Amersham, England); rotenone (Sigma Chemical Company, Saint-Louis, Missouri, U.S.A.); mersalyl, acid form (Mann Research Laboratories, New York, U.S.A.).

Preloading of the Mitochondria

Rat-heart mitochondria were prepared according to Tyler and Gonze [9] and loaded with L-malate at 0 °C as described previously [8]. The various concentrations of internal L-malate were obtained by washings in large volume [8]. Internal oxoglutarate could not be detected in such preparations.

Experimental Assays

The incubation medium contained 15-mM KCl, 5-mM MgCl₂, 2-mM EDTA, 50-mM Tris · Cl (pH 7.4), 22.5-mM mannitol and 7.5-mM sucrose (both derived from the stock mitochondrial suspension); the mitochondria preloaded with malate were incubated for 1 min at 4 °C in 1 ml of the incubation medium in the presence of 4 μg rotenone, 1 μmol sodium arsenite and 0.2 μmol mersalyl. Labelled 2-oxoglutarate (or malonate) was then added to the suspension for a further incubation period of 5, 15 or 25 s at 4 °C. The mitochondria were finally separated from the incubation mixture by rapid centrifugation in an Eppendorf microcentrifuge (model 3200). For further experimental details see [8] and the legends of the figures.

The radioactivities were determined in a Packard liquid-scintillation counter with Insta-Gel (Packard) as scintillation medium.

The exchanges were measured under 27 experimental conditions: at three concentrations of the internal substrate (L-malate), three concentrations of the external substrate (2-oxoglutarate or malonate) and three concentrations of the external reaction product (L-malate). Their initial rates, as well as

subsequent calculations were determined as described in [8]; they were referred to the tritium space of the mitochondrial pellet (see [8]).

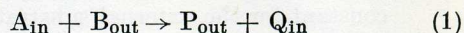
The concentration of internal malate was determined enzymatically with malate dehydrogenase.

Justification

The essential conditions for such a kinetic study have already been discussed [8] and may be summarised as follows: (a) the anions should not be metabolised, (b) the incubation medium should not be contaminated by the internal anions (in the control experiments), and the matrix space should not contain external anions at the onset of the experiments, and (c) the magnitude of the exchange should be kept low.

Theory

The exchanges were treated as two-substrate two-product reactions [Eqn (1)] in which the product P_{out} is the translocated substrate A_{in} and the product Q_{in} is the translocated substrate B_{out}:



This is justified by the fact that the oxoglutarate translocator catalyses a simple 1:1 exchange-diffusion [11] between 2-oxoglutarate and a dicarboxylate. In a preceding analysis [8] of initial rates in the absence of reaction products, the conclusion had been reached that the exchange reactions followed the law expressed by Eqn (2):

$$1/v = \frac{1}{V} \left(1 + \frac{K_b}{[B]} + \frac{K_a}{[A]} + \frac{K_a K_b}{[A][B]} \right). \quad (2)$$

If the mechanism of the reaction is the so-called 'rapid-equilibrium random bi-bi', as proposed in [8], the kinetic constants are dissociation constants: K_b , dissociation constant of EB and EAB (into EA + B); K_a , dissociation constant of EA and EAB (into EB + A); and $V = k[E_t]$.

This paper reports the effect of various concentrations of P_{out} on the initial rate of the exchange A_{in}/B_{out}.

Assuming the 'rapid-equilibrium random bi-bi' with a 'dead-end complex' EAP (inhibition is then mixed dead-end and product inhibition), Eqn (2) becomes, following the indications of Cleland [12]:

$$1/v = \frac{1}{V} \left\{ 1 + \frac{K_a}{[A]} + \frac{K_b}{[B]} \left(1 + \frac{[P]}{K_p} \right) + \frac{K_a K_b}{[A][B]} \left(1 + \frac{[P]}{K_p} \right) \right\} \quad (3a)$$

where K_p is the dissociation constant of the complexes EP and EAP (into EA + P).

Eqn (3a) may also be written:

$$1/v = \frac{1}{V} \left(1 + \frac{K_a}{[A]}\right) \left(1 + \frac{[P]}{K_p}\right) \frac{K_b}{[B]} + \frac{1}{V} \left(1 + \frac{K_a}{[A]}\right) \quad (3b)$$

or

$$1/v = \frac{1}{V} \left(1 + \frac{K_b}{[B]}\right) \left\{1 + \frac{[P]}{K_p \left(1 + \frac{[B]}{K_b}\right)}\right\} \frac{K_a}{[A]} + \frac{1}{V} \left(1 + \frac{K_b}{[B]}\right) \left\{1 + \frac{[P]}{K_p \left(1 + \frac{[B]}{K_b}\right)}\right\} \quad (3c)$$

If [A] and [P] are constant, and if [B] is variable, then the apparent-maximum rates are independent of the concentration of P and the Michaelis constant for B is equal to $K_b \left(1 + \frac{[P]}{K_p}\right)$. Thus the inhibition by external product will be competitive when [B] is varied.

If [B] and [P] are constant, and if [A] is variable, the Michaelis constant for A is unaffected by the concentration of P and the apparent-maximum rates (V_{app}) for the various concentrations of B decrease when the concentration of P increases, according to the following equation:

$$V_{app} = V \left/ \left(1 + \frac{K_b}{[B]}\right) \left\{1 + \frac{[P]}{K_p \left(1 + \frac{[B]}{K_b}\right)}\right\} \right. \quad (4)$$

Thus the inhibition by external product will be non-competitive when [A] is varied.

Data Processing

A mathematical treatment has been devised which enables calculation of the various kinetic parameters as well as their standard deviation (see Appendix).

RESULTS

The kinetics of the product inhibition of the two exchange reactions are presented in a series of double-reciprocal plots in which the points are arranged as a function of the internal-anion concentration (part A) and as a function of external-anion concentration (part B). The exchanges were carried out in the presence of three concentrations of external malate (product inhibitor): 0, 5 or 10 μ M.

Fig.1: external 2-oxo[5- 14 C]glutarate/internal L-malate; Fig.2: external 2-oxo[5- 14 C]glutarate plus 5- μ M L-malate/internal L-malate; Fig.3: external 2-oxo[5- 14 C]glutarate plus 10- μ M L-malate/internal L-malate; Fig.4: external [2- 14 C]malonate/internal L-malate; Fig.5: external [2- 14 C]malonate plus 5- μ M L-malate/internal L-malate; Fig.6: external [2- 14 C]malonate plus 10- μ M L-malate/internal L-malate.

The figures show linear relationships between v^{-1} on the one hand, and $[S_{in}]^{-1}$ or $[S_{out}]^{-1}$ on the other hand, even in the presence of external product. In each half-figure the four straight lines have a common intercept with the axis of the abscissae in the presence or in the absence of external product. As predicted by the theory, it clearly appears that the value of K^{-1} for internal malate is unaffected by the presence of the external product whereas the

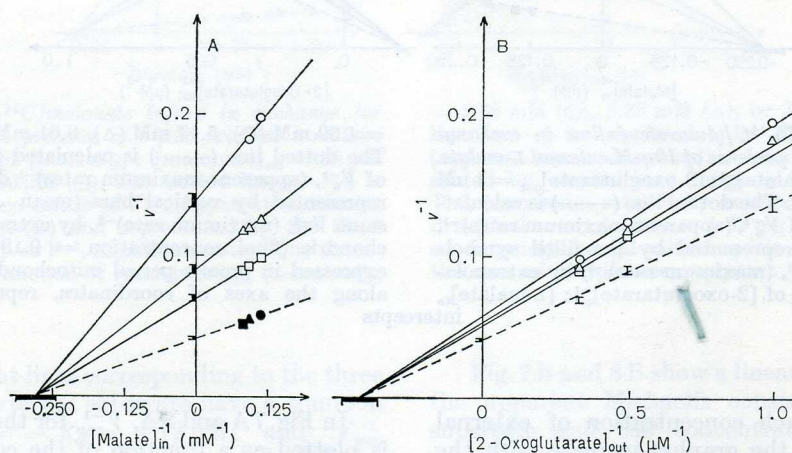


Fig.1. Kinetics of 2-oxo[5- 14 C]glutarate influx in exchange for internal L-malate. (A) v^{-1} as a function of $[\text{malate}]_{in}^{-1}$; $[\text{2-oxoglutarate}]_{out} = 1 \mu\text{M}$ (O), $2 \mu\text{M}$ (Δ), or $3 \mu\text{M}$ (\square). The dotted line (---) is calculated from the three values of V_a^{-1} , (apparent-maximum rates) $^{-1}$, determined in (B) and represented by the filled symbols (\bullet , \blacktriangle , \blacksquare); it gives V^{-1} , (maximum rate) $^{-1}$, by extrapolation. (B) v^{-1} as a function of $[\text{2-oxoglutarate}]_{out}^{-1}$; $[\text{L-malate}]_{in} = 8.94 \text{ mM}$ (O), 10.92 mM

(Δ), or 12.23 mM (\square). The dotted line (---) is calculated from the three values of V_a^{-1} , (apparent-maximum rate) $^{-1}$, determined in (A) and represented by vertical bars (mean \pm S.D.); it gives the same V^{-1} , (maximum rate) $^{-1}$, by extrapolation. Heart mitochondria (final concentration = $0.21 \text{ mg protein/ml}$); v is expressed in $\text{pmol/s per } \mu\text{l mitochondria}$; the thick marks, along the axes of coordinates, represent \pm S.D. of the intercepts

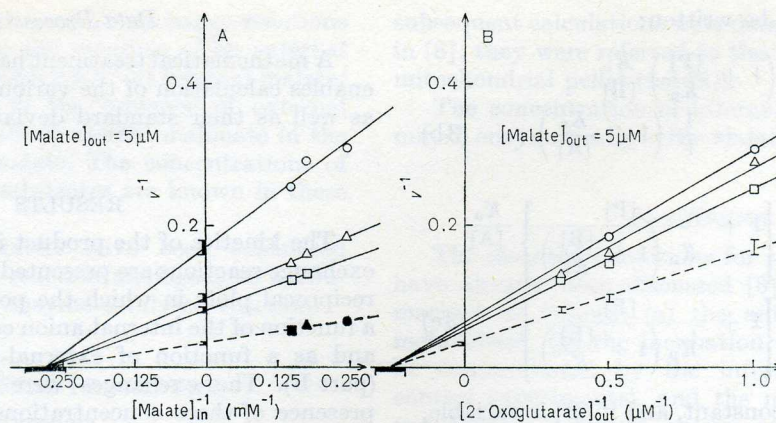


Fig. 2. Kinetics of 2-oxo[5- ^{14}C]glutarate influx in exchange for internal L-malate in the presence of 5- μM external L-malate. (A) v^{-1} as a function of $[\text{malate}]_{\text{in}}^{-1}$; $[\text{2-oxoglutarate}]_{\text{out}} = 1 \mu\text{M}$ (\circ), 2 μM (Δ), or 3 μM (\square). The dotted line (----) is calculated from the three values of V_{app}^{-1} , (apparent-maximum rates) $^{-1}$, determined in (B) and represented by the filled symbols (\bullet , \blacktriangle , \blacksquare); it gives V^{-1} , (maximum rate) $^{-1}$, by extrapolation. (B) v^{-1} as a function of $[\text{2-oxoglutarate}]_{\text{out}}^{-1}$; $[\text{L-malate}]_{\text{in}}$

$= 4.07 \text{ mM}$ (\circ), 5.71 mM (Δ), or 6.83 mM (\square). The dotted line (----) is calculated from the three values of V_{app}^{-1} , (apparent-maximum rates) $^{-1}$, determined in (A) and represented by vertical bars (mean \pm S.D.); it gives the same V^{-1} , (maximum rate) $^{-1}$, by extrapolation. Heart mitochondria (final concentration = 0.16 mg protein/ml); v is expressed in pmol/s per μl mitochondria; the thick marks, along the axes of coordinates, represent \pm S.D. of the intercepts

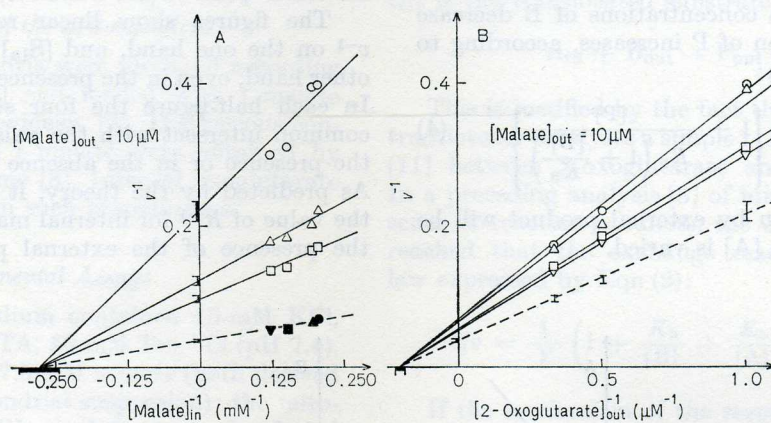


Fig. 3. Kinetics of 2-oxo[5- ^{14}C]glutarate influx in exchange for internal L-malate in the presence of 10- μM external L-malate. (A) v^{-1} as a function of $[\text{malate}]_{\text{in}}^{-1}$; $[\text{2-oxoglutarate}]_{\text{out}} = 1 \mu\text{M}$ (\circ), 2 μM (Δ), or 3 μM (\square). The dotted line (----) is calculated from the four values of V_{app}^{-1} , (apparent-maximum rates) $^{-1}$, determined in (B) and represented by the filled symbols (\bullet , \blacktriangle , \blacksquare , \blacktriangledown); it gives V^{-1} , (maximum rate) $^{-1}$, by extrapolation. (B) v^{-1} as a function of $[\text{2-oxoglutarate}]_{\text{out}}^{-1}$; $[\text{L-malate}]_{\text{in}}$

$= 4.89 \text{ mM}$ (\circ), 5.17 mM (Δ), 6.61 mM (\square), or 8.20 mM (∇). The dotted line (----) is calculated from the three values of V_{app}^{-1} , (apparent-maximum rates) $^{-1}$ determined in (A) and represented by vertical bars (mean \pm S.D.); it gives the same V^{-1} , (maximum rate) $^{-1}$, by extrapolation. Heart mitochondria (final concentration = 0.19 mg protein/ml); v is expressed in pmol/s per μl mitochondria; the thick marks, along the axes of coordinates, represent \pm S.D. of the intercepts

values of V_{app}^{-1} for each concentration of external substrate (part A on the graphs) increase with the concentration of external product. On the other hand the value of K^{-1} for the external substrate, oxoglutarate or malonate, decreases when the concentration of external malate increases.

The Michaelis constants and maximum rates of the exchanges together with their standard deviations are summarised in Tables 1 and 2.

In Fig. 7A and 8A, V_{app}^{-1} for the internal substrate is plotted as a function of the concentration of the external product, for each fixed concentration of external substrate. The equation of the linear relationship obtained can be deduced from Eqn (3c) and is:

$$1/V_{\text{app}} = \frac{1}{V} \left(1 + \frac{K_b}{[B]} \right) \left\{ 1 + \frac{[P]}{K_p \left(1 + \frac{[B]}{K_b} \right)} \right\}$$

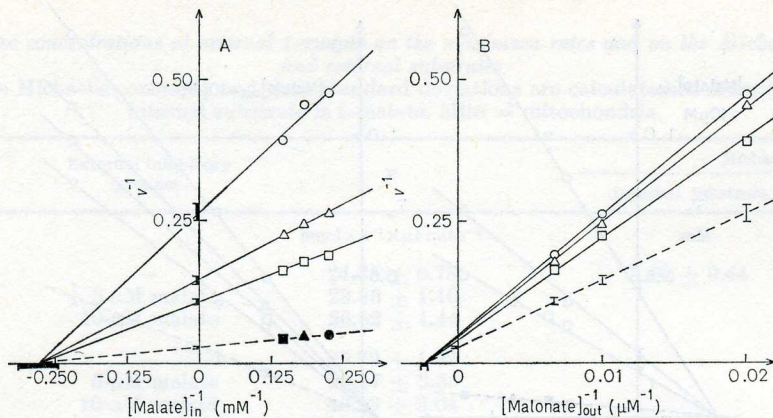


Fig. 4. Kinetics of $[2\text{-}^{14}\text{C}]$ malonate influx in exchange for internal *L*-malate. (A) v^{-1} as a function of $[\text{malate}]_{\text{in}}^{-1}$; $[\text{malonate}]_{\text{out}} = 50 \mu\text{M}$ (O), $100 \mu\text{M}$ (Δ), or $150 \mu\text{M}$ (\square). The dotted line (---) is calculated from the three values of V_{a}^{-1} , (apparent-maximum rates)⁻¹, determined in (B) and represented by the filled symbols (●, ▲, ■); it gives V^{-1} , (maximum rate)⁻¹, by extrapolation. (B) v^{-1} as a function of $[\text{malonate}]_{\text{out}}^{-1}$; $[\text{L-malate}]_{\text{in}} = 4.43 \text{ mM}$ (O), 5.49 mM (Δ), or 6.84 mM (\square).

The dotted line (---) is calculated from the three values of V_{a}^{-1} , (apparent-maximum rates)⁻¹, determined in (A) and represented by vertical bars (mean \pm S.D.); it gives the same V^{-1} , (maximum rate)⁻¹, by extrapolation. Heart mitochondria (final concentration = $2.14 \text{ mg protein/ml}$); v is expressed in pmol/s per μl mitochondria; the thick marks, along the axes of coordinates, represent \pm S.D. of the intercepts

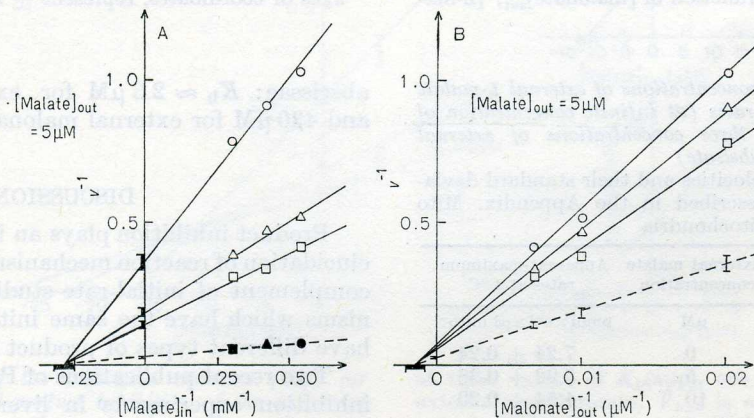


Fig. 5. Kinetics of $[2\text{-}^{14}\text{C}]$ malonate influx in exchange for internal *L*-malate in the presence of $5\text{-}\mu\text{M}$ external *L*-malate. (A) v^{-1} as a function of $[\text{malate}]_{\text{in}}^{-1}$; $[\text{malonate}]_{\text{out}} = 50 \mu\text{M}$ (O), $100 \mu\text{M}$ (Δ), or $150 \mu\text{M}$ (\square). The dotted line (---) is calculated from the three values of V_{a}^{-1} , (apparent-maximum rates)⁻¹, determined in (B) and represented by the filled symbols (●, ▲, ■); it gives V^{-1} , (maximum rate)⁻¹, by extrapolation. (B) v^{-1} as a function of $[\text{malonate}]_{\text{out}}^{-1}$; $[\text{L-malate}]_{\text{in}} = 1.86 \text{ mM}$ (O), 2.38 mM (Δ), or 3.30 mM (\square).

The dotted line (---) is calculated from the three values of V_{a}^{-1} , (apparent-maximum rates)⁻¹, determined in (A) and represented by vertical bars (mean \pm S.D.); it gives the same V^{-1} , (maximum rate)⁻¹, by extrapolation. Heart mitochondria (final concentration = $1.62 \text{ mg protein/ml}$); v is expressed in pmol/s per μl mitochondria; the thick marks, along the axes of coordinates, represent \pm S.D. of the intercepts

The three straight lines corresponding to the three concentrations of external substrate have a common intercept at $[\text{P}] = -K_{\text{p}} \approx -12 \mu\text{M}$, and $V_{\text{app}}^{-1} = V^{-1} \approx (25 \text{ pmol} \times \text{s}^{-1} \text{ per } \mu\text{l mitochondria})^{-1}$ for the exchange malate_{in}/oxoglutarate_{out} and $V^{-1} \approx (36 \text{ pmol} \times \text{s}^{-1} \text{ per } \mu\text{l mitochondria})^{-1}$ for the exchange malate_{in}/malonate_{out}. Each line intercepts with the axis of the abscissae at a point where

$$[\text{P}] = -K_{\text{p}}(\text{app}) = -K_{\text{p}} \left(1 + \frac{[\text{B}]}{K_{\text{b}}} \right).$$

Fig. 7 B and 8 B show a linear relationship between the apparent Michaelis constant for the external substrate and the concentration of the external product, as expected from Eqn 3 b:

$$K_{\text{app}} = K_{\text{b}} \left(1 + \frac{[\text{P}]}{K_{\text{p}}} \right).$$

The intersect of this straight line with the axis of the abscissae is $-K_{\text{p}} \approx -12 \mu\text{M}$ in either exchange.

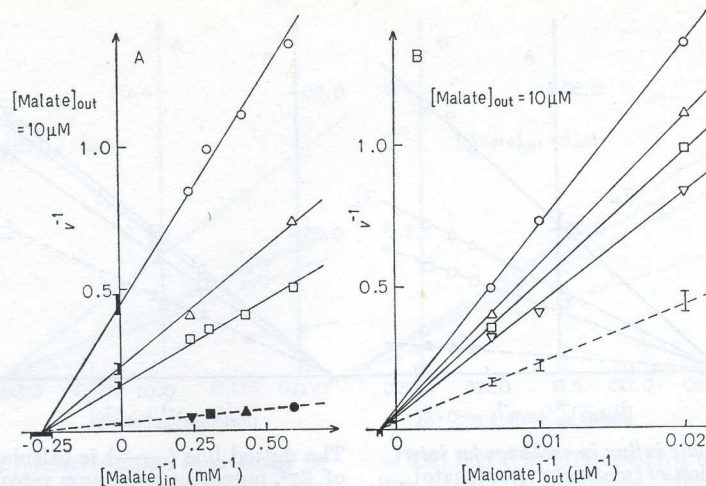


Fig. 6. Kinetics of $[2-^{14}\text{C}]$ malonate influx in exchange for internal L-malate in the presence of $10\text{-}\mu\text{M}$ external L-malate. (A) v^{-1} as a function of $[\text{malate}]_{\text{in}}^{-1}$; $[\text{malonate}]_{\text{out}} = 50\text{ }\mu\text{M}$ (O), $100\text{ }\mu\text{M}$ (Δ), or $150\text{ }\mu\text{M}$ (\square). The dotted line (----) is calculated from the four values of V_{b}^{-1} , (apparent-maximum rates) $^{-1}$, determined in (B) and represented by the filled symbols (\bullet , \blacktriangle , \blacksquare , \blacktriangledown); it gives V^{-1} (maximum rate) $^{-1}$, by extrapolation. (B) v^{-1} as a function of $[\text{malonate}]_{\text{out}}^{-1}$; $[\text{L-ma-}$

late] $_{\text{in}} = 1.68\text{ mM}$ (O), 2.32 mM (Δ), 3.28 mM (\square), or 4.18 mM (\blacktriangledown). The dotted line (----) is calculated from the three values of V_{a}^{-1} , (apparent-maximum rates) $^{-1}$, determined in (A) and represented by vertical bars (mean \pm S.D.); it gives the same V^{-1} , (maximum rate) $^{-1}$, by extrapolation. Heart mitochondria (final concentration = $1.41\text{ mg protein/ml}$); v is expressed in $\text{pmol/s per } \mu\text{l mitochondria}$; the thick marks, along the axes of coordinates, represent \pm S.D. of the intercepts

Table 1. Influence of three concentrations of external L-malate on the apparent-maximum rates (at infinite concentration of internal L-malate and at three concentrations of external substrate)

The apparent-maximum velocities and their standard deviations are calculated as described in the Appendix. Mito = mitochondria

External labelled substrate	External malate concentration	Apparent-maximum rates at $4\text{ }^{\circ}\text{C}$
	μM	$\text{pmol} \times \text{s}^{-1} \times \mu\text{l mito}^{-1}$
1- μM Oxoglutarate	0	7.24 ± 0.24
	5	5.92 ± 0.36
	10	4.54 ± 0.29
2- μM Oxoglutarate	0	11.04 ± 0.34
	5	10.27 ± 0.52
	10	8.20 ± 0.41
3- μM Oxoglutarate	0	14.41 ± 0.46
	5	12.34 ± 0.62
	10	10.46 ± 0.52
50- μM Malonate	0	3.77 ± 0.20
	5	2.78 ± 0.21
	10	2.25 ± 0.17
100- μM Malonate	0	6.83 ± 0.35
	5	5.50 ± 0.43
	10	4.60 ± 0.38
150- μM Malonate	0	9.35 ± 0.46
	5	7.11 ± 0.61
	10	6.16 ± 0.46

$K_{\text{p}}(\text{app})$ varies linearly with the concentration of the external substrate as shown in Fig. 7C and 8C. $-K_{\text{b}}$ is the intersect of this line with the axis of the

abscissae: $K_{\text{b}} \approx 2.3\text{ }\mu\text{M}$ for external oxoglutarate and $430\text{ }\mu\text{M}$ for external malonate.

DISCUSSION

Product inhibition plays an important rôle in the elucidation of reaction mechanisms. It is the necessary complement of initial-rate studies [12]. Two mechanisms which have the same initial-rate pattern may have different types of product inhibition.

Two recent publications of Palmieri *et al.* describe inhibition experiments in liver mitochondria. The first one [4] concerns the dicarboxylate translocator and reports experiments where essential experimental conditions are not properly known, as discussed in a preceding paper [8]. The second one [7] shows competitive inhibition of the entrance of tricarboxylate by other possible substrates of the tricarboxylate translocator (other tricarboxylates, dicarboxylates or phosphoenolpyruvate).

The present paper describes experiments in which two exchanges catalysed by the oxoglutarate translocator have been measured with only this translocator active and under conditions where it has been possible to vary the concentrations of internal and external substrates and the concentration of external reaction product. The study of internal-product inhibition is technically impossible.

a) The external product inhibits the exchange in a competitive way when external substrate is varied. The inhibition constant determined for the external product, K_{p} (Fig. 7 B and 8 B), is equal to the already

Table 2. Influence of three concentrations of external L-malate on the maximum rates and on the Michaelis constants for internal and external substrates

The maximum rates, the Michaelis constants and their standard deviations are calculated as described in the Appendix. The internal substrate is L-malate. Mito = mitochondria

External substrate	External inhibitory product	V pmol \times s $^{-1}$ \times μ l mito $^{-1}$	Michaelis constants	
			Internal substrate mM	External substrate μ M
Oxoglutarate	—	24.35 \pm 0.78	3.60 \pm 0.44	2.34 \pm 0.34
	5- μ M malate	28.86 \pm 1.10		3.84 \pm 0.79
	10- μ M malate	26.82 \pm 1.44		4.82 \pm 0.38
Malonate	—	35.79 \pm 1.92		424 \pm 36
	5- μ M malate	39.57 \pm 3.35		657 \pm 278
	10- μ M malate	40.13 \pm 3.04		840 \pm 62

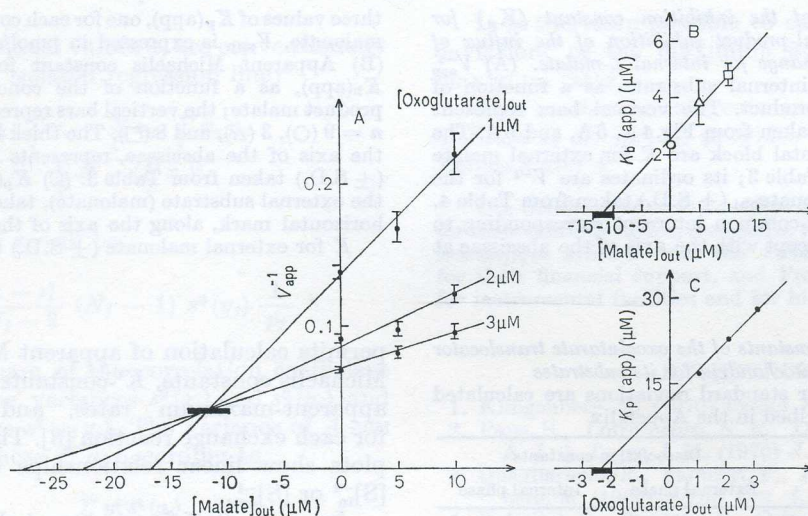


Fig. 7. Determination of the inhibition constant (K_p) for L-malate in the external-product inhibition of the influx of 2-oxo[5- 14 C]glutarate in exchange for internal L-malate. (A) V_{app}^{-1} at infinite $[\text{malate}]_{in}$, internal substrate, as a function of $[\text{malate}]_{out}$, external product. The vertical bars represent mean \pm S.D. of V_{app}^{-1} taken from Fig. 1 A, 2 A, and 3 A. The abscissae of the horizontal block are K for external malate (\pm S.D.) taken from Table 3; its ordinates are V^{-1} for the exchange malate $_{in}$ /oxoglutarate $_{out}$ (\pm S.D.) taken from Table 4. The three lines have a common intercept corresponding to K_p , whereas they intercept with the axis of the abscissae taken from Table 3

at three values of $K_p(\text{app})$, one for each concentration of external oxoglutarate. V_{app} is expressed in pmol/s per μ l mitochondria. (B) Apparent Michaelis constant for external oxoglutarate, $K_b(\text{app})$, as a function of the concentration of external product malate; the vertical bars represent the mean \pm S.D.; $n = 9$ (O), 3 (Δ), and 5 (\square). The thick horizontal mark, along the axis of the abscissae, represents K for external malate (\pm S.D.) taken from Table 3. (C) $K_p(\text{app})$ as a function of the external substrate (oxoglutarate), taken from (A). The thick horizontal mark, along the axis of the abscissae, represents K for external oxoglutarate (\pm S.D.) taken from Table 3

determined (Table 3) dissociation constant of the corresponding external-substrate \cdot translocator complex.

b) The external product inhibits the exchange in a non-competitive way when internal substrate is varied. The K_p determined here (Fig. 7A and 8A) have the same value as in (a).

These results are in perfect agreement with the proposed mechanism (rapid-equilibrium random bi-bi) and a mixed dead-end and product inhibition.

It should be realised however that the inhibition pattern observed could also be explained by a steady-state ordered bi-bi mechanism where the only binary complexes of the translocator would be those including the external anions. It must also be supposed that the product does not form a dead-end complex EAP. This last restriction is not consistent with the fact that this complex must exist in the exchange of a substrate for itself; three such exchanges exist and have been studied [8].

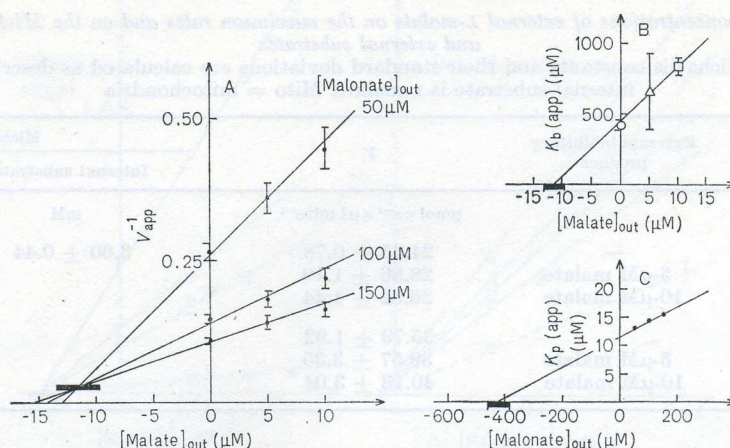


Fig. 8. Determination of the inhibition constant (K_p) for L-malate in the external-product inhibition of the influx of [^{14}C]malonate in exchange for internal L-malate. (A) V_{app}^{-1} at infinite $[\text{malate}]_{\text{in}}$, internal substrate, as a function of $[\text{malate}]_{\text{out}}$, external product. The vertical bars represent mean \pm S.D. of V_{app}^{-1} taken from Fig. 4A, 5A, and 6A. The abscissae of the horizontal block are K for external malate (\pm S.D.) taken from Table 3; its ordinates are V^{-1} for the exchange $\text{malate}_{\text{in}}/\text{malonate}_{\text{out}}$ (\pm S.D.) taken from Table 4. The three lines have a common intercept corresponding to K_p , whereas they intercept with the axis of the abscissae at

three values of $K_p(\text{app})$, one for each concentration of external malonate. V_{app} is expressed in pmol/s per μl mitochondria. (B) Apparent Michaelis constant for external malonate, $K_b(\text{app})$, as a function of the concentration of external product malate; the vertical bars represent the mean \pm S.D.; $n = 9$ (O), 3 (Δ), and 8 (\square). The thick horizontal mark, along the axis of the abscissae, represents K for external malate (\pm S.D.) taken from Table 3. (C) $K_p(\text{app})$ as a function of the external substrate (malonate), taken from (A). The thick horizontal mark, along the axis of the abscissae, represents K for external malonate (\pm S.D.) taken from Table 3

Table 3. Dissociation constants of the oxoglutarate translocator of rat-heart mitochondria for its substrates. The K -values and their standard deviations are calculated as described in the Appendix

Anions	Dissociation constants	
	External phase	Internal phase
	μM	mM
2-Oxoglutarate	2.34 ± 0.34	1.48 ± 0.21
Malate	11.6 ± 1.7	3.60 ± 0.44
Malonate	424 ± 36	5.90 ± 0.84
Succinate	141 ± 22	

Table 4. Maximum rates of the exchange reactions catalysed by the oxoglutarate translocator of rat-heart mitochondria. The maximum rate (at 4°C) and their standard deviations are calculated as described in the Appendix

External anion	Internal anion		
	2-Oxoglutarate	Malate	Malonate
	$\text{pmol} \times \text{s}^{-1} \times \mu\text{l mitochondria}^{-1}$		
2-Oxoglutarate	25.0 ± 0.8	24.4 ± 0.8	22.6 ± 2.2
Malate	18.8 ± 1.1	33.3 ± 2.5	31.2 ± 3.0
Malonate	27.7 ± 1.0	35.8 ± 1.9	29.3 ± 3.0
Succinate	20.5 ± 0.8	37.7 ± 2.1	38.1 ± 4.0

APPENDIX

Double-reciprocal plots of initial rates *versus* substrate concentrations were analysed according to the method of Florini and Vestling [12] which

permits calculation of apparent Michaelis constants, Michaelis constants, K' -constants for each substrate, apparent-maximum rates, and maximum rates for each exchange reaction [8]. The double-reciprocal plots show linear relationships between v^{-1} *versus* $[\text{S}]_{\text{in}}^{-1}$ or $[\text{S}]_{\text{out}}^{-1}$.

In each half-figure reported in [8], the four straight lines had a common intersect on the axis of the abscissae. Thus $K_{\text{app}} = K = K'$. The experimental results also showed that the K -value for a substrate on one side of the membrane was unaffected by the nature of the counter-ion. It was therefore possible to calculate K^{-1} accurately from the extrapolation of 9 straight lines (three for each of the three exchanges) to the $[\text{S}]^{-1}$ -axis. This was achieved by imposing a common intersect with the $[\text{S}]^{-1}$ -axis, to the straight lines calculated by the method of least squares.

In the following development, x represents v^{-1} and y represents $[\text{S}]^{-1}$. Thus, if the linear regressions have a common intersect with the y -axis, the value of which is unknown *a priori*, the equation of the j^{th} regression line is:

$$y_j^* = A + B_j x$$

The y_j^* is the predicted value of y for each value of x . The intersect (A) with the y -axis, common to the regression lines, and the slopes (B_j), characteristic of each line, are symbolised by capital letters by opposition to the individual a_j and b_j -values which

are the parameters of those regression lines, to which no common intersect would be imposed.

There are N pairs of experimental data (x_{ij}, y_{ij}) = coordinates of the point i on the straight line j which are distributed in N_j points associated with the j^{th} regression line. The A (i.e. $-K^{-1}$) is then expressed by:

$$A = \frac{\sum_j p_j a_j}{\sum_j p_j}$$

where the statistical weight, p_j , are:

$$p_j = N_j - \frac{(\sum_i x_{ij})^2}{\sum_i x_{ij}^2}$$

and where the individual values a_j are conventionally calculated for each isolated regression line:

$$a_j = \frac{\sum_i x_{ij}^2 \cdot \sum_i y_{ij} - \sum_i x_{ij} \cdot \sum_i x_{ij} y_{ij}}{N_j \cdot \sum_i x_{ij}^2 - (\sum_i x_{ij})^2}$$

The variance of a_j will be:

$$s^2(a_j) = \frac{1 - r_j^2}{N_j - 2} (N_j - 1) s^2(y_j) \frac{1}{p_j}$$

where r_j^2 is the square of the correlation coefficient calculated from the variances $s^2(x_j)$ and $s^2(y_j)$ and from the covariance $s^2(x_j y_j)$. The variance of A can be deduced from those of a_j according to:

$$s^2(A) = \frac{\sum_j p_j^2 s^2(a_j)}{(\sum_j p_j)^2}$$

The standard deviation of A is $s(A)$ and the standard deviation of A^{-1} (i.e. K) is $s(A^{-1}) \approx s(A)/A^2$.

The values of the slopes B_j , characterising each straight line which have a common intersect with the y -axis are calculated from:

$$B_j = \frac{\sum_i x_{ij} y_{ij} - A \sum_i x_{ij}}{\sum_i x_{ij}^2}$$

where A is the common intersect on the y -axis.

The variance of B_j can be expressed as a function of $s^2(a_j)$ and $s^2(A)$ by:

$$s^2(B_j) = \frac{p_j s^2(a_j)}{\sum_i x_{ij}^2} + \left[\frac{\sum_i x_{ij}}{\sum_i x_{ij}^2} \right]^2 s^2(A)$$

Maximum velocities are given by $-B_j/A$ and their standard deviations can be deduced from the following considerations.

The variance of a predicted value of y_j^* for a value of x on the j^{th} regression line can be calculated from:

$$s^2(y_j^*) = \left(1 - \frac{2x\bar{x}_j}{x_j^2}\right) s^2(A) + x^2 s^2(B_j)$$

where $x = -A/B$. What is needed is the variance of a value of x for a particular value of y . This can be obtained from the following relation which links the two standard deviations:

$$s(x_j) \approx \frac{s(y_j^*)}{B_j}$$

The standard deviation of x_j^{-1} may then be obtained from:

$$s(x_j^{-1}) \approx s(x_j)/x_j^2$$

It is therefore possible to calculate the standard deviations of the maximum and of the apparent-maximum rates.

This mathematical treatment, applied to the data of Sluse *et al.* [8,13], provides the results given in Tables 3 and 4.

Our thanks are due to Laurette Bertrand and Eli Dethier for their skilful technical assistance, the *Fonds de la Recherche Scientifique Médicale* and the *Fondation Philippe Lefebvre* for their financial support, and Prof. H. van Cauwenberge for instrumental facilities and for his help.

REFERENCES

1. Klingenberg, M. (1970) *Essays Biochem.* 6, 119-159.
2. Papa, S., Lofrumento, N. E., Quagliariello, E., Meyer, A. J. & Tager, J. M. (1970) *J. Bioenerg.* 1, 287-307.
3. Quagliariello, E., Palmieri, F., Prezioso, G. & Klingenberg, M. (1969) *FEBS Lett.* 4, 251-254.
4. Palmieri, F., Prezioso, G., Quagliariello, E. & Klingenberg, M. (1971) *Eur. J. Biochem.* 22, 66-74.
5. Robinson, B. H. & Williams, G. R. (1970) *Biochim. Biophys. Acta*, 216, 63-70.
6. Robinson, B. H., Williams, G. R. & Halperin, M. L. (1971) *J. Biol. Chem.* 246, 5280-5286.
7. Palmieri, F., Stipani, I., Quagliariello, E. & Klingenberg, M. (1972) *Eur. J. Biochem.* 26, 587-594.
8. Sluse, F. E., Ranson, M. & Liébecq, C. (1972) *Eur. J. Biochem.* 25, 207-217.
9. Tyler, D. D. & Gonze, J. (1967) *Methods Enzymol.* 10, 75-77.
10. Papa, S., Lofrumento, N. E., Kanduc, D., Paradies, G. & Quagliariello, E. (1971) *Eur. J. Biochem.* 22, 134-143.
11. Cleland, W. W. (1963) *Biochim. Biophys. Acta*, 67, 173-187.
12. Florini, J. R. & Vestling, C. S. (1957) *Biochim. Biophys. Acta*, 25, 575-578.
13. Sluse, F. E. & Derome, A. (1972) *Arch. Int. Physiol. Biochim.* 80, 619-621.

F. E. Sluse and C. Liébecq
Laboratoire de Biochimie et de Physiologie Générale
Institut Supérieur d'Éducation Physique de l'Université
Rue des Bonnes-Villes 1, B-4000 Liège, Belgium

G. Goffart's private address:
Rue Edouard-Wacken 36, B-4000 Liège, Belgium